Systematic identification of novel regulatory interactions controlling biofilm formation in the bacterium *Escherichia coli*

Gerardo Ruiz Amores[1], Aitor de las Heras[2,3], Ananda Sanches-Medeiros[1], Alistair Elfick[2,3] and Rafael Silva-Rocha[1]*

[1]FMRP - University of São Paulo, Ribeirão Preto, SP, Brazil
[2]Institute for Bioengineering, School of Engineering, University of Edinburgh, Edinburgh, UK
[3]SynthSys Research Centre, University of Edinburgh, Edinburgh, UK

Running Title: Regulatory network for biofilm formation in bacteria
Keywords: Biofilm formation in bacteria, regulatory network, global regulation

_____

*Correspondence to: Rafael Silva-Rocha
                         Faculdade de Medicina de Ribeirão Preto, Universidade de São Paulo
                         Av. Bandeirantes, 3.900. CEP: 14049-900.
                         Ribeirão Preto, São Paulo, Brazil
                         Tel.: +55 16 3602 3107; Fax: +55 16 3633 6840
                         E-mail: silvarochar@gmail.com

ABSTRACT

Here, we investigated novel interactions of three global regulators of the network that controls biofilm formation in the model bacterium *Escherichia coli* using computational network analysis, an *in vivo* reporter assay and physiological validation experiments. We were able to map critical nodes that govern planktonic to biofilm transition and identify 8 new regulatory interactions for CRP, IHF or Fis responsible for the control of the promoters of *rpoS*, *rpoE*, *flhD*, *fliA*, *csgD* and *yeaJ*. Additionally, an *in vivo* promoter reporter assay and motility analysis revealed a key role for IHF as a repressor of cell motility through the control of FliA sigma factor expression. This investigation of first stage and mature biofilm formation indicates that biofilm structure is strongly affected by IHF and Fis, while CRP seems to provide a fine-tuning mechanism. Taken together, the analysis presented here shows the utility of combining computational and experimental approaches to generate a deeper understanding of the biofilm formation process in bacteria.

_____

INTRODUCTION

Bacteria shift from their free-swimming lifestyle to adopt a community structure to benefit from the micro-environment created in a biofilm [1], gaining protection against hazardous substances, and leading in some cases, to antibiotic resistance [1, 2, 3]. It is well-understood that when differentiating from the planktonic to a biofilm structure bacteria transit through specific stages, with each functional stage accompanied by changes to expression of specific genes of the flagella-biofilm regulatory network [1, 2, 3]. In *Escherichia coli*, the complex transcriptional regulatory network of flagella function and curli fimbriae production, the principal biofilm structure indicator, has been investigated in various reports [4, 5, 6, 7]. In this organism, the process is controlled by the RpoS sigma factor and FlhDC regulator. These master regulators receive major regulatory inputs from c-di-GMP, cAMP and ppGpp, which are modulated by a series of environmental and physiological stresses [8, 9, 10]. In this sense, the *flhDC* genes are expressed at post-exponential phase and their products control more than 60 genes involved in flagella synthesis and related functions, such as chemotaxis [11]. Also at stationary phase, the general stress response master regulator RpoS is produced and controls

2

74   over 500 genes in a highly complex regulatory network [7]. Therefore, the interplay between those master regulators

75   and downstream-activated genes modulates the complex transition between planktonic and biofilm stages.

76   In the case of planktonic bacteria, mainly found in the exponential phase, flagella maintenance is due to the

77   activation of effector molecules such as FliA sigma factor. Whilst, at stationary phase, biofilm formation is initiated by

78   increasing levels in the secondary messenger c-di-GMP, as well as expression and activation of *rpoS,* which in turn

79   leads to the activation of *csgD* [5, 12]. Additionally, there are alternative mechanisms that involve different key genes of

80   the biofilm pathway, also leading to *csgD* activation and scale-up of curli fiber production; such as CpxR and ClpX

81   which play a complex dual role during bacterium development to inhibit or activate both programs [8, 10, 13].

82   Undoubtedly, the interplay between these molecules acts to modulate the proper execution of the flagella-biofilm

83   program [14, 15]. Experimentally, the transition between flagella and biofilm formation is evaluated using a "batch cells"

84   assay, in which cells grow and attach to the chemically-inert surface of a microliter dish under static conditions,

85   generating a biofilm in an "aquatic environment". Additionally, the "macro-colonies" assay allows a bacterial

86   population to grow over extended periods of time on agar plates, leading to striking morphological patterns,

87   resembling biofilms growing in biological materials.

88   While hundreds of reports have dissected the molecular mechanisms leading to biofilm formation in several bacterial

89   groups, a full understanding the dynamics of the complex regulatory network controlling planktonic to biofilm

90   transition still lies out of reach. This is particularly true since most studies analyzed the effect of particular regulators

91   on the expression of specific sets of genes, without addressing the complexity of the network using a more

92   systematic approach. In particular, since a few global regulators (GRs) are able to control most of the genes in

93   genome of *E. coli* [16], it is anticipated that the role of these transcriptional factors in the biofilm formation network is

94   rather underestimated. GRs are expressed or activated differentially during growth or under specific input signals [17].

95   Specifically, CRP is related to the control of metabolic processes in bacteria and it is differentially activated by

96   substrates [18], while IHF (growth rate dependent) and Fis (expressed at early exponential phase) are dual nucleoid

97   associated proteins (NAPs) that can work both as activators and repressors [19, 20]. During the transition from motile

98   cells to biofilm structure, a mixture of different developmental stages occur. In this sense, small molecules and GRs

3

99   direct the activation of signaling proteins that are sensed by neighboring cells, coordinating the construction of this

100   complex community structure [14, 15]. Therefore, mapping hidden interactions in the flagella-biofilm regulatory network

101   would provide a better understanding of this developmental-like program and provide new targets for intervention

102   and/or engineering [21, 22].

103   In this work, we used computational tools and molecular biology, together with microbiology approaches to

104   investigate the effect of the GRs CRP, IHF and Fis on the *E. coli* flagella-biofilm network. First, to analyze regulatory

105   interactions already reported, we reconstructed the flagella-biofilm transcriptional regulatory network *in silico* using

106   previous data and we analyzed its structure. Next, by using promoter expression assays, we mapped novel

107   regulatory interactions between the three GRs and key genes controlling biofilm formation. Finally, novel regulatory

108   interactions mapped using this approach were added to the original network to generate an enhanced appreciation of

109   biofilm formation. The general strategy used here is depicted in **Fig. 1**. These results suggest that IHF and Fis are

110   important modulators of the process while CRP seems to exert a fine-tuning effect. Additionally, using motility,

111   adherence and biofilm formation assays, we validated key regulatory effects observed using transcriptional fusions.

112   All together, the systematic investigation presented here adds new understanding of the complex regulatory program

113   that controls biofilm formation in *E. coli*, revealing a novel player in this network.

114   **RESULTS AND DISCUSSION**

115   ***In silico* analysis of the regulatory network controlling planktonic to biofilm transition in *E. coli***

116   To reconstruction the flagella-biofilm regulatory network, information regarding the transcriptional regulation of *E. coli*

117   was gathered from scientific articles and compiled with that from RegulonDB [23] and KEGG DB [24]. The resulting

118   network consisted of 37 nodes representing the connections between different transcription factors (TFs), GRs and

119   small molecules **(Fig. 2)**. The degree analysis (which shows the most connected nodes) of the flagella-biofilm

120   transcriptional regulatory network identified three major hubs, *rpoS*, *flhD* and *csgD* (**Fig. S1A**). The betweenness and

121   edge betweenness analysis which provides information about the most important nodes and paths in the network,

122   shows that from 37 nodes, 8 seem to be the principal effectors that modulate the proper gene expression of the

123   network (*rpoS, csgD,* c-di-GMP*, rpoE, cpxR, clpX, flhD, fliA*). Interestingly, *rpoS* is the main effector in the network

124   and it is modulated by different inputs. From those, c-di-GMP presents high betweenness and edge connection

125   values (**Fig. 2**). From the 37 nodes, *rpoD* and CRP were the main nodes, which exert more out-regulatory signals to

126   other nodes, while all others possessed fewer out-connections (**Fig. S1B**). Additionally, this analysis shows three

127   paths that seem to be important to maintain balance in the network. The first critical connection that maintains

128   flagella-biofilm program equilibrium lies between *rpoS* and *rpoE*, activating both *fliA* for motility and its repressor

129   *matA*, to eventually develop adherence. Secondly, *rpoS* with the TF *cpxR*, which modulates *rpoE*, but also has an

130   important connection with the TF *nsrR*, which represses *fliA* expression. Thirdly, the activation of *clpX* ATPase by

131   *rpoS* that exerts *flhD* inhibition at post-transcriptional and/or post-translational levels [25]. From the analysis presented

132   here, we selected ten genes in order to perform a systematic investigation of the effect of CRP, IHF and Fis, which

133   are among the main GRs of the regulatory network of *E. coli* [26]. We expected that this approach would reveal some

134   hidden interactions controlling the critical nodes of the flagella-biofilm network. The selected genes of interest were

135   *rpoS, rpoE, csgD, cpxR, flhD, fliA, matA, ompR, adrA and yeaJ*. In order to analyze the promoter activity of the

136   selected genes, the promoter regions of the genes were cloned upstream of a GFPlva reporter system [27] and used to

137   transform wild-type and *Δihf* and *Δfis* mutant strains of *E. coli*. As control, an empty reporter plasmid and a strong

138   synthetic promoter named BBa_J23100 (http://parts.igem.org/Part:BBa_J23100, here referred as *Pj100*) were also

139   used to transform the same strains (**Fig. S2**). The 36 reporter strains were then analyzed as presented in the next

140   section.

141

142   **CRP, IHF and Fis modulate promoters of *rpoS*, *rpoE* and *flhD* master regulators**

143   We started our investigation by considering the three putative master regulators of the transition from planktonic to

144   biofilm phases. The sigma factor RpoS has been proposed as a main regulator of the flagella-biofilm network [7,8], in

145   agreement with our network analysis. Thus, we were interested to understand the effect of these three GRs on the

146   promoter region of the *rpoS* gene. For this, overnight cultures of *E. coli* wild-type strain carrying the transcriptional

147   *PrpoS::GFPlva* fusion were diluted 1:100 in fresh M9 minimal medium supplemented with glycerol as sole carbon

148 source, and GFP fluorescence was measured at 20 minute time intervals over 8 hours at 37˚C. As can be seen in

149 **Fig. 3A**, the analyzed promoter presented a growth-phase-dependent activity with increased activity toward the end

150 of the growth curve. When the same reporter system was analyzed in *E. coli Δihf* and *Δfis* mutant strains, we

151 observed a significant increase in promoter activity in the absence of IHF and a strong activity in the absence of Fis

152 (**Fig. 3A left panel**, red and green lines, respectively). These data strongly suggest that IHF and Fis GRs are acting

153 to repress the *rpoS* promoter. To understand the role of CRP over the *rpoS* promoter region, we employed the

154 glucose inducible CCR system to down-modulate the activity of CRP by adding glucose in the same experimental

155 conditions as described above [28]. When the three reporter strains were analyzed in the presence of 0.4% glucose,

156 we observed the same general expression profile as in **Fig. 3A left panel** but a remarkably reduced promoter activity

157 (**Fig. 3A right panel**), confirming the previously reported positive role of CRP on the *rpoS* promoter [29]. Additionally,

158 since the synthetic constitutive promoter (*Pj100*) was not significantly affected in the strains and conditions used (**Fig.**

159 **S2**), we concluded that the effects observed for *rpoS* promoter are true regulatory events taking place at this

160 element.

161 When we analyzed the activity of the *rpoE* promoter, which controls the expression of a sigma factor linking RpoS

162 activity with flagella genes (**Fig. 2**), we observed a strong increase in promoter activity in the *Δihf* and *Δfis* strains of

163 *E. coli* when compared to the wild-type strain (**Fig. 3B left panel**), indicating that IHF and Fis have a negative effect

164 on the activity of this promoter. However, contrary to the observation for *rpoS*, the addition of glucose (**Fig. 3b right**

165 **panel**) to the media (which inhibits CRP activity) did not result in any significant change in *rpoE* promoter activity.

166 After investigating the activity of *rpoS* and *rpoE* promoters, we analyzed the promoter of *flhD* gene, which encodes a

167 master regulator of flagellar genes and of the flagella-related *fliA* sigma factor [30]. Using the same experimental

168 conditions as described above, we first observed that *flhD* promoter activity has a strong growth-dependence, with

169 activity increasing during the growth curve when assayed in the wild-type strain of *E. coli* (**Fig. 3C left panel**). When,

170 we assayed the promoter activity in *Δihf* and *Δfis* mutant strains, we observed a similar expression profile as in the

171 wild-type, with the exception that in both strains the initial promoter activity was significantly higher than in the wild-

172 type. When we assayed promoter response in the three strains in the presence of glucose (to trigger CRP

173   inactivation), activity was strongly impaired in all strains (**Fig. 3C right panel**), confirming the reported role of CRP as

174   activator of *flhD* expression [31].

175   **Novel regulatory effects for CRP, IHF and Fis exerted on *csgD*, *fliA* and *yeaJ* promoters**

176   Once we had investigated the effect of the GRs of flagella to biofilm transition, we decided to analyze the promoters

177   of genes related to biofilm formation and an additional lower flagella regulator (*fliA*). CsgD is a central protein related

178   to, and an indicator of, biofilm formation [12, 32]. When we analyzed the activity of *csgD* promoter in the wild-type strain,

179   we observed a peak of expression at about 200 min of growth with a reduced activity later in the growth phase (**Fig.**

180   **4A left panel**). Investigating this promoter in *Δihf* and *Δfis* mutants, we observed a strong decay in promoter activity,

181   indicating that both proteins positively modulate the activity of the promoter. Moreover, when we added glucose to

182   the growth media (**Fig. 4A right panel**), we observed a generalized decay in promoter activity in all three strains,

183   indicating a positive role of CRP for this promoter. Reflecting on these results, it is interesting to note that, while CRP

184   and IHF have been reported as positive regulators of the *csgD* promoter [33, 34], the positive effect of Fis has never

185   been demonstrated before.

186   In the case of the *fliA* gene that codes a sigma factor specifically related to flagella genes, analysis of promoter

187   activity in both wild-type and *Δfis* mutant strains revealed a very low level of activity throughout the growth curve,

188   both in the presence and absence of glucose (**Fig. 4B**). However, in the *Δihf* mutant strain, this promoter displays a

189   strong increase (30-fold) in activity in the absence of glucose (left panel), while this level was lower when glucose

190   was added (right panel). Since *fliA* expression is dependent on FlhD [30], the observed decay of *fliA* promoter activity

191   during growth in the presence of glucose could be the result of a cascade process, with the apparent IHF repression

192   of this promoter suggesting a previously unreported regulatory interaction. To test the direct effect of IHF on FliA, we

193   identified two putative binding sites for this global regulator at *fliA* promoter **Fig. S3A**. We then constructed a mutant

194   version of this promoter with 11 point mutations that fully abolish both sites and tested this new variant as before. As

195   shown in **Fig. S3B**, expression of the mutated version of *fliA* promoter was low in the wild-type and *Δfis* mutant

196   strains at the same level as the original promoter, and displayed a higher activity in the *Δihf* mutant, both in the

197   absence and presence of glucose. These data suggest that the effect of IHF on *fliA* promoter is indirect.

198   We next analyzed the effect of GRs on the expression of *yeaJ*, a diguanylate cyclase coding gene, which modulates

199   the levels of c-di-GMP in the cell. In *E. coli*, deletion of *yeaJ* results in strains with reduced motility at 37 ºC [8],

200   however no regulatory proteins have been demonstrated to play a role in the expression of this gene. The expression

201   profile of the *yeaJ* promoter in wild-type and Δ*ihf* mutants strains showed a strong peak of activity at 200 min of

202   experiment (**Fig. 4C**). However, when this promoter was assayed in the Δ*fis* mutant, we observed a significant

203   decrease in promoter activity, indicating that the Fis regulator could play a positive role in its expression.

204   Furthermore, addition of glucose to the growth media (**Fig. 4C right panel**) resulted in an increase in the promoter

205   activity in the first minutes of growth, suggesting the existence of additional, potentially CRP-dependent, regulatory

206   mechanisms at this promoter. Finally, the additional three promoters selected for investigation (from *adrA*, *cpxR* and

207   *ompR* genes, **Fig. S4**) displayed maximal activity very similar to that of the negative control (the empty reporter

208   vector, pMR1 in **Fig. S2**), which precludes unequivocal conclusions concerning their regulation.

209   **Reconstruction and analysis of the regulatory network with novel interactions**

210   In order to generate fresh insight into the regulatory network controlling biofilm formation in *E. coli*, we added the new

211   regulatory interactions identified in the previous sections to the network from **Fig. 2.** For this, the effect of CRP, IHF

212   and Fis over the promoter regions obtained by our promoter activity assay was transformed into activation or

213   inhibition links. From the 27 interactions tested, we suggested 8 new interactions, and were able to confirm 5

214   described interactions (**Table S1**). We integrated these new interactions into the network and re-performed the

215   centrality measurements. Using this approach, we observed that the integration of the experimental data changed the

216   topology of the network, while maintaining the three major hubs identified (**Fig. S5A**). Yet, the out-degree analysis

217   showed that *rpoD,* CRP, IHF, and Fis in minor degree are the main nodes exerting the most out-connections to all

218   other nodes (**Fig. S5B**), while the edge betweeness analysis indicates that, upon the addition of the new interactions,

219   the critical nodes of the network remain the same (**Fig. 5**). Taken together, these data suggest the existence of

220   previously unidentified regulatory interactions in the biofilm regulatory network that play a critical role in the planktonic

221   to biofilm transition.

222   **Phenotypic consequences of loss of GRs for the planktonic and biofilm stages of _E. coli_**

223   Flagella play an important function during the different developmental phases of biofilm formation such as attachment

224   at a surface, as well as bacterial cell cohesion within the biofilm [2, 30]. Therefore, we were interested in understanding

225   the effect of the GRs CRP, IHF and Fis on the flagella function. As it can be seen in **Fig. 6**, after 24h of incubation in

226   a low agar plate, _E. coli_ BW25113 wild-type strain showed reduced motility in the absence of glucose. However,

227   analysis of the Δ_ihf_ strain in similar conditions revealed a strong motile phenotype, with this effect more apparent

228   after 24h of incubation with full spreading over the plate observed (**Fig. S6**). Finally, under similar conditions, the Δ_fis_

229   strain presented reduced motility, which is more evident at 24h. It is important to notice that addition of glucose to the

230   media generated a general decrease in motility of all strains (**Figs. 6** and **S6**, right panels). Interestingly, the

231   observed strong phenotypic effect of Δ_ihf_ on the motility of _E. coli_ can be traced directly to the strong increase of _fliA_

232   promoter activity in this mutant strain, since FliA sigma factor controls several genes related to flagella formation in

233   this organism [35].

234   We next analyzed the capability of the different strains to attach to a solid surface, which is indicative of early biofilm

235   formation, using the protocol described by O'Toole _et al_., 2011. For this, we performed the experiments at 30 ºC and

236   37 ºC, since different reports have used different temperatures [36, 37]. In general, _E. coli_ cells adhered to the wall of the

237   96-well plates in all conditions. At 37˚C, two- or three-fold increases in biofilm yields were observed when compared

238   with _E. coli_ cells cultured at 30˚C, as can be seen by comparing the biofilm indexes in **Fig. 7A**. In general terms, the

239   Δ_ihf_ mutant strain of _E. coli_ displayed decreased adhesion at both temperatures, which is in agreement with the

240   increased motility observed for this strain in **Fig. 6**. By the same token, adhesion of the Δ_fis_ mutant strain at 37 ºC

241   was significantly increased when compared to the wild-type, which could be due to the reduced motility observed

242   before. In most of the cases, the general adhesion observed for the strains was decreased in the presence of

243   glucose, with the exception of the adhesion level of Δ_ihf_ mutant at 30 ºC. These data suggest that, at 37˚C, CRP and

9

244   IHF are important effectors to activate the adherence program. They also suggest that Fis is acting as a repressor of

245   the early biofilm program, since in its absence, motility is higher at 37 ºC. Altogether, adherence yields are better

246   when induced at 37˚C than at 30˚C, and the three GRs CRP, IHF and Fis participate differentially to regulate the

247   adherence capabilities of *E. coli.*

248   As depicted in **Fig. S7**, all the strains were capable of developing biofilm structures at 30 ºC and 37 ºC in the

249   presence or absence of glucose, as previously reported. In general, *E. coli* cells grown at 30 ºC produced a biofilm

250   structure resembling that reported for 28 ºC, while those grown at 37 ºC conditions showed a more visually complex

251   biofilm structure with three morphologically distinct zones, as reported by Serra *et al.*, 2013 (**Fig. 7B**). More explicitly,

252   in wild-type cells a concentric ring delineates zone 3, which presents an intense red color suggesting curli formation

253   by the different layers of stationary phase cells. Zone 2 represents the intrinsic capability of wild-type community to

254   produce wrinkles and curli. Finally, zone 1 presents weak red color, an indicative of bacteria at exponential phase

255   related with colony expansion but not with curli production [7]. In the presence of glucose, the biofilm structure formed

256   by the wild-type strain presented slight differences. When we analyzed the *Δihf* mutant strain, we observed a

257   significant reduction in the colony size and degree of pigmentation (that could be related to lower curli production)

258   when compared to the two other strains (**Fig. 7B**). This size reduction can be evidenced by the systematic decrease

259   in the three zones of the colony in this strain. Yet, analysis of biofilm formation in this strain in the presence of

260   glucose showed a recovery in colony size generated by a high expansion of zone 1, while pigmentation was

261   apparently not affected. Finally, the analysis of *Δfis* mutant strain revealed a colony where the zone 1 (expansion

262   zone) could not be detected. Additionally, this strain presented a darker zone 3, which could be indicative of higher

263   production of curli fimbriae than wild-type strain, with addition of glucose to the growth media only generated small

264   changes in the colony such as an apparent reduction in size.

265   Altogether, morphology assays have shown that IHF and Fis GRs are important contributors to proper biofilm

266   development, as could be indicated by drastic changes in the three well-characterized zones in these mutants. In

267   contrast, the role of CRP protein (which was indirectly assayed by the addition of glucose to the media) during

268   mature biofilm formation could not be dependably inferred, since the change in the nutritional state of the colonies

269 could have a strong impact in the process. Taken together, these data indicate that these GRs could have an

270 important role in the final biofilm structure in *E. coli* that could be the result of the detected change in gene expression

271 of key regulatory elements in the planktonic to biofilm regulatory network.

272 **Conclusions**

273 The work presented here describes the systematic investigation of the regulatory interaction mediated by GRs during

274 the transition from planktonic to biofilm in the bacterium *E. coli*. While several works have addressed this issue

275 before, data generated has been fragmented and few targets have been investigated at each time. The systematic

276 investigation used here allowed the identification of novel interactions mediated by CRP, Fis and IHF. More

277 importantly, the modulation of some critical nodes, such as *fliA* by IHF, could explain the strong phenotypic effects

278 observed for motility and attachment assays, as this regulator has also been found to be a modulator of genes

279 involved in the biofilm program as *rpoS*, *matA* and *csgD* [33, 38, 39, 40]. The molecular mechanism involved in the different

280 phases of biofilm formation by IHF remains to be determined. However, in this work, we present evidence that IHF is

281 a key element to biofilm formation by modulating gene expression level of the flagella-biofilm program, suggesting

282 that IHF could be a good candidate to disrupt/engineer bacterial biofilm structure. Here, we also demonstrated that

283 Fis plays a more major role in the biofilm formation network than anticipated, both using promoter assays as well as

284 physiological tests. The evidence in this study indicates that, CRP, IHF and Fis are important effectors that modulate

285 the flagella-biofilm network. Interestingly, no condition in this study shows absence of motility or biofilm formation,

286 suggesting that, while these GRs are important modulators of these processes, they are not essential genes to

287 suppress completely the flagella-biofilm program. Additionally, it has been demonstrated that bacteria without the

288 main effectors *rpoS* or *csgD* (also *rpoE*, *csgB*, *flhDC* or *fliA*) are still capable of producing a biofilm [7, 41]. Altogether,

289 the high plasticity observed in the flagella-biofilm program clearly shows that the network has evolved the robustness

290 to compensate for the loss of critical nodes, indicating the importance of this program for bacterial survival. Finally,

291 the systematic identification of novel connections for a specific network will allow prediction of the behavior of the

292 biological system in the absence of different TFs. It opens the possibility of using genetic engineering to achieve a

293 balanced connectivity between synthetic circuits and the entire bacterial network when performing a specific task. In

294   other words, that rational interactive synthetic circuits can operate in accordance with the natural network of a

295   specific organism, thereby allowing enhanced performance of a desired biological task.

296

297

298   **EXPERIMENTAL PROCEDURES**

299   **Bacterial strains, media and growth conditions**

300   The list of bacterial strains, plasmids and primers is presented in **Table1**. *Escherichia coli* wild-type (BW25113) or

301   strains genetically depleted of IHF or Fis GRs [42] were used as the host of all plasmids. *E. coli* DH5α or DH10b were

302   used as cloning strains. DNA of *E. coli* BW25113 and MG1655 were used as templates. *E. coli* cells were grown in

303   Luria Broth (LB) or M9 minimal media (6.4g/L $Na_2HPO_4 \cdot 7H_2O$, 1.5g/L KH_2PO_4, 0.25g/L NaCl, 0.5g/L NH_4Cl)

304   supplemented with 2mM $MgSO_4$, 0.1mM $CaCl_2$, 0.1mM casamino acids, and 1% glycerol or 0.4% glucose as the

305   carbon source. Chloramphenicol was added (34 µg/mL) to ensure plasmid maintenance. Cells were grown at 37°C

306   with constant shaking at 220 rpm overnight.

307   **Plasmid construction**

308   Plasmids and primers used in this work are listed on Table 2 and 3 respectively. As a control of all experiments we

309   transformed *E. coli* BW25113 wild-type and mutant strains with an empty pMR1 vector [27] and pMR1-Pj100. To

310   analyze the signal integration of GRs at the studied genes, we amplified the promoter regions by PCR and cloned

311   into pMR1 vector using standard protocols [43]. DNA from *E. coli* BW25113 wild-type was used as a template for all

312   constructions except for *flhD* promoter, for which *E. coli* MG1655 was used. PCR was performed using 50 ng of DNA

313   template with 50pmol of each primer (purchased from Sigma and extended) and 1U Phusion® High-Fidelity DNA

314   Polymerase (New England Biolabs M0530L) in a 50 µl reaction volume. Initial denaturation was at 98˚C for five

315   minutes; subsequently, amplification was done over 30 cycles at 98˚C, 60˚C and 72˚C, each with duration of 30

316   seconds. The final extension step was performed at 72˚C for ten minute . All PCR products were gel purified and

317   cloned as EcoRI/BamHI fragments in pMR1, previously digested with the same enzymes. The resulting plasmids

318   were DNA sequence verified and correct plasmids were used to transform *E. coli* BW25113 (wild-type), *E. coli*

319   JW1702 (*Δihf*) and *E. coli* JW3229 (*Δfis*).

320

Promoter activity assay

322   For promoter activity measurements, single colonies of wild-type and mutant *E. coli* strains harboring the different

323   plasmids were picked from fresh plates. Each strain was inoculated and grown overnight at 37 °C in 2 mL of M9

324   medium with glycerol or glucose containing chloramphenicol with shaking at 225 rpm. Stationary phase cultures were

325   diluted to a final optical density (OD) of 0.05 in 200 μL of M9 medium containing either glycerol or glucose as

326   required, and supplemented with chloramphenicol. Cell growth and GFP fluorescence was quantified every 20

327   minutes over an 8 hr incubation at 37 °C using Victor X3 plate reader (PerkinElmer, Waltham, Massachusetts, USA).

328   Under these conditions, all strains presented similar growth rates (**Fig. S8**). Data were analyzed from at least three

329   biological samples, arbitrary units were calculated by dividing GFP-corrected by OD600-corrected, subsequently, the

330   mean and standard error for each promoter was calculated and graphed using Microsoft Excel and R software.

Bacteria motility assay

332   The effect of GRs on motility was evaluated as following. *E. coli* wild-type or mutant strains harboring pMR1 plasmid

333   were grown overnight at 37˚C on LB plates. Inoculation of a single colony onto motility plates (tryptone 1%, NaCl

334   0.25%, agar 0.3% and when indicated glucose was added) was done by using a toothpick [44]. The motility halos were

335   measured at 18h and 24h. Each strain was evaluated in triplicate from independent plates.

Biofilm formation in liquid media

337   Biofilm formation was assayed using the Microtiter Dish Biofilm Formation Assay [45]. Single colonies of *E. coli* wild-

338   type or mutant strains harboring all the constructions were grown overnight at 37˚C in M9 supplemented with glycerol

339   or glucose. The cultures were diluted 1:100 in 200μl of fresh M9 media with either glycerol or glucose. A 96-well plate

340   was incubated at 37˚C for 72h, after which cells were gently washed four times with distilled water and left at room

341   temperature for 15 minutes with 200µL of crystal violet 0.1% w/v solution. Subsequently, vigorous washing was

342   performed with distilled water (four times) and the plates left to dry at room temperature for 24h. Finally, 200µL acetic

343   acid 30% w/v was added and after 15 minutes, the solution was transferred to a new plate and Optical Density at

344   550nm was measured in FLUOstar Omega (BMG Labtech) plate reader. All the culture dilutions, staining and

345   quantification steps were performed by using procedures developed for a robotic platform called Edwin [46]. Data from

346   biological triplicates were analyzed by Microsoft Excel software. Average values and standard deviation was

347   determined.

Biofilm formation in solid media

349   Biofilm morphology was evaluated by Congo red assay [47]. Chloramphenicol was added during all steps to ensure

350   plasmid maintenance. Wild-type and mutant *E. coli* strains with pMR1 plasmid were grown overnight at 37˚C on LB

351   agar plates. Single colonies were picked and grown for 14h at 37˚C on 1ml LB at 220rpm. The cultures were washed

352   twice with $MgSO_4$ and resuspended in M9 media with either glycerol or glucose as required, to an OD at 600nm (~

353   0.5). 5 µL drop of each culture was added into YESCA-CR plates [48]. YESCA media (1 g/L yeast extract, 20 g/L agar)

354   was complemented with Congo red 50 µg/ml diluted in KPi buffer (50 mM potassium phosphate buffer, pH 7.2, 28.9

355   mM KH_2PO_4, 21.1 mM K_2HPO_4 in water), where indicated glucose was added at 0.4% final concentration. YESCA-

356   CR seeded plates were allowed to dry in a sterile environment and, left to grow at 37˚C. Biofilm development was

357   followed (documented) for 6 days using a fluorescence stereoscope (Leica MZ16). Biological triplicate images were

358   analyzed by ImageJ and prisma software was used to determine the statistical significance of the experiments by

359   using one-way ANOVA.

Network Construction

361   To generate the transcriptional regulatory network that will define our genes of interest, we gathered information from

362   research articles that contained information on genes that modulate the transition between planktonic to biofilm

363   formation. Eventually, the data were compared with information available at Regulon DB, EcoCyc DB and Kegg

14

364   pathway DB. Cytoscape 3.4.1 was used to generate the transcriptional network with slight modifications [49]. Briefly,

365   we transformed our mined data into activation or inhibition statements for each of the partner molecules. Secondly, to

366   construct the network graph, we used Cytoscape 3.4.1 in which different connections were added to each node on

367   the collected data. Next, networks were analyzed using different algorithms, such as degree, out-degree,

368   betweenness centrality by using Cytoscape 3.4.1 software. Finally, we transformed our GFP dynamics gene

369   expression experimental results into functional interactions (inhibits or activates). Results with same function as

370   reported were maintained without changes in the rewired network, while those with different activity were changed in

371   the network. During the data collection from the literature, some TFs were reported with dual effect (activation and

372   repression) for the same target gene. For instance, *rpoS* expression was reported to be activated but also inactivated

373   by the CRP global regulator [50, 51, 52]. Additionally, most of the genes that were reported as being regulated by different

374   TFs, but in the web-databases the same gene did not present a *cis*-element to any TFs. To overcome those

375   constrains we considered for the network that any TF, master regulator, global regulator, small molecule or RNAs

376   could be a node. This last, despite being gathered, were not included because RNA-node analysis of regulatory gene

377   expression significantly increases the complexity of the network [12, 53] and because of the complex requirements of

378   molecular tools to evaluate this topic. For edges direction analysis, we considered the activation or inhibition most

379   reported, or both when divergent reports were found. The data were plotted in a power-law graph using an organic

380   algorithm to give cluster visualization generating the transcriptional regulatory network of both planktonic and biofilm

381   structure. Furthermore, we performed degree analysis in order to present a general view of the most connected

382   nodes, followed by edge and node betweenness analysis [54] in order to disclose the main effectors and the logic

383   pathway that could describe the network. Finally, we also performed the out degree analysis at the integrated

384   network to identify the potential talkative nodes.

385

386   **ACKNOWLEDGMENTS**

392

393   **AUTHOR CONTRIBUTIONS**

394   G.R.A. and R.S.R. conceived the work. G.R.A., A.dH. and A.S.M. performed the experiments. G.R.A., A.dH. and

395   A.M.S. analyzed the data. G.R.A. and R.S.R. drafted the manuscript. A.dH. and A.E. corrected the manuscript. A.E.

396   and R.S.R. provided funding for the execution of the work. All authors read and approved the manuscript.

397   **COMPETING FINANCIAL INTEREST**

398   The authors declare no competing financial interest.

399   **MATERIAL & CORRESPONDENCE**

400   Correspondence and material request should be addressed to Rafael Silva Rocha.

401   **ADDITIONAL INFORMATION**

402   Supplementary Information accompanies this paper online.

403

REFERENCES

1. Beloin C, Roux A, Ghigo JM. Escherichia coli biofilms. *Current topics in microbiology and immunology* **322**, 249-289 (2008).

2. Laverty G, Gorman SP, Gilmore BF. Biomolecular Mechanisms of Pseudomonas aeruginosa and Escherichia coli Biofilm Formation. *Pathogens* **3**, 596-632 (2014).

3. Solano C, Echeverz M, Lasa I. Biofilm dispersion and quorum sensing. *Curr Opin Microbiol* **18**, 96-104 (2014).

4. Martinez-Antonio A, Janga SC, Thieffry D. Functional organisation of Escherichia coli transcriptional regulatory network. *J Mol Biol* **381**, 238-247 (2008).

5. Ogasawara H, Yamamoto K, Ishihama A. Role of the biofilm master regulator CsgD in cross-regulation between biofilm formation and flagellar synthesis. *J Bacteriol* **193**, 2587-2597 (2011).

6. Sanchez-Torres V, Hu H, Wood TK. GGDEF proteins YeaI, YedQ, and YfiN reduce early biofilm formation and swimming motility in Escherichia coli. *Appl Microbiol Biotechnol* **90**, 651-658 (2011).

7. Serra DO, Richter AM, Klauck G, Mika F, Hengge R. Microanatomy at cellular resolution and spatial order of physiological differentiation in a bacterial biofilm. *MBio* **4**, e00103-00113 (2013).

8. Pesavento C*, et al.* Inverse regulatory coordination of motility and curli-mediated adhesion in Escherichia coli. *Genes & development* **22**, 2434-2446 (2008).

9. Sommerfeldt N, Possling A, Becker G, Pesavento C, Tschowri N, Hengge R. Gene expression patterns and differential input into curli fimbriae regulation of all GGDEF/EAL domain proteins in Escherichia coli. *Microbiology* **155**, 1318-1331 (2009).

10. Valentini M, Filloux A. Biofilms and Cyclic di-GMP (c-di-GMP) Signaling: Lessons from Pseudomonas aeruginosa and Other Bacteria. *J Biol Chem* **291**, 12547-12555 (2016).

11. Chevance FF, Hughes KT. Coordinating assembly of a bacterial macromolecular machine. *Nat Rev Microbiol* **6**, 455-465 (2008).

12. Mika F, Hengge R. Small RNAs in the control of RpoS, CsgD, and biofilm architecture of Escherichia coli. *RNA Biol* **11**, 494-507 (2014).

17

443   13.   Hengge R. Stationary-Phase Gene Regulation in Escherichia coli §. *EcoSal Plus* **4**, (2011).
444

445   14.   Petrova OE, Sauer K. Escaping the biofilm in more than one way: desorption, detachment or dispersion.
446   *Curr Opin Microbiol* **30**, 67-78 (2016).
447

448   15.   Srivastava S, Bhargava A. Biofilms and human health. *Biotechnology letters* **38**, 1-22 (2016).
449

450   16.   Martínez-Antonio A, Collado-Vides J. Identifying global regulators in transcriptional regulatory networks in
451   bacteria. *Curr Opin Microbiol* **6**, 482-489 (2003).
452

453   17.   Ishihama A. Prokaryotic genome regulation: multifactor promoters, multitarget regulators and hierarchic
454   networks. *FEMS Microbiol Rev* **34**, 628-645 (2010).
455

456   18.   Shimizu K. Metabolic Regulation and Coordination of the Metabolism in Bacteria in Response to a Variety of
457   Growth Conditions. *Advances in biochemical engineering/biotechnology* **155**, 1-54 (2016).
458

459   19.   McLeod SM, Johnson RC. Control of transcription by nucleoid proteins. *Curr Opin Microbiol* **4**, 152-159
460   (2001).
461

462   20.   Dillon SC, Dorman CJ. Bacterial nucleoid-associated proteins, nucleoid structure and gene expression. *Nat
463   Rev Microbiol* **8**, 185-195 (2010).
464

465   21.   Hall-Stoodley L, Costerton JW, Stoodley P. Bacterial biofilms: from the natural environment to infectious
466   diseases. *Nat Rev Microbiol* **2**, 95-108 (2004).
467

468   22.   Wood TK, Hong SH, Ma Q. Engineering biofilm formation and dispersal. *Trends Biotechnol* **29**, 87-94
469   (2011).
470

471   23.   Huerta AM, Salgado H, Thieffry D, Collado-Vides J. RegulonDB: a database on transcriptional regulation in
472   Escherichia coli. *Nucleic Acids Res* **26**, 55-59 (1998).
473

474   24.   Wixon J, Kell D. The Kyoto encyclopedia of genes and genomes--KEGG. *Yeast* **17**, 48-55 (2000).
475

476   25.   Tomoyasu T*, et al.* The ClpXP ATP-dependent protease regulates flagellum synthesis in Salmonella
477   enterica serovar typhimurium. *J Bacteriol* **184**, 645-653 (2002).
478

479   26.   Martinez-Antonio A, Collado-Vides J. Identifying global regulators in transcriptional regulatory networks in
480   bacteria. *Curr Opin Microbiol* **6**, 482-489 (2003).

481

27. Guazzaroni ME, Silva-Rocha R. Expanding the logic of bacterial promoters using engineered overlapping operators for global regulators. *ACS synthetic biology* **3**, 666-675 (2014).

28. Amores GR, Guazzaroni ME, Silva-Rocha R. Engineering Synthetic cis-Regulatory Elements for Simultaneous Recognition of Three Transcriptional Factors in Bacteria. *ACS Synth Biol*, (2015).

29. Venturi V. Control of rpoS transcription in Escherichia coli and Pseudomonas: why so different? *Mol Microbiol* **49**, 1-9 (2003).

30. Liu X, Matsumura P. The FlhD/FlhC complex, a transcriptional activator of the Escherichia coli flagellar class II operons. *J Bacteriol* **176**, 7345-7351 (1994).

31. Kalir S, Alon U. Using a quantitative blueprint to reprogram the dynamics of the flagella gene network. *Cell* **117**, 713-720 (2004).

32. Chirwa NT, Herrington MB. CsgD, a regulator of curli and cellulose synthesis, also regulates serine hydroxymethyltransferase synthesis in Escherichia coli K-12. *Microbiology* **149**, 525-535 (2003).

33. Ogasawara H, Yamada K, Kori A, Yamamoto K, Ishihama A. Regulation of the Escherichia coli csgD promoter: interplay between five transcription factors. *Microbiology* **156**, 2470-2483 (2010).

34. Gerstel U, Park C, Romling U. Complex regulation of csgD promoter activity by global regulatory proteins. *Mol Microbiol* **49**, 639-654 (2003).

35. Barembruch C, Hengge R. Cellular levels and activity of the flagellar sigma factor FliA of Escherichia coli are controlled by FlgM-modulated proteolysis. *Mol Microbiol* **65**, 76-89 (2007).

36. Gualdi L, Tagliabue L, Bertagnoli S, Ierano T, De Castro C, Landini P. Cellulose modulates biofilm formation by counteracting curli-mediated colonization of solid surfaces in Escherichia coli. *Microbiology* **154**, 2017-2024 (2008).

37. White-Ziegler CA, Um S, Perez NM, Berns AL, Malhowski AJ, Young S. Low temperature (23 degrees C) increases expression of biofilm-, cold-shock- and RpoS-dependent genes in Escherichia coli K-12. *Microbiology* **154**, 148-166 (2008).

38. Hengge-Aronis R. Recent insights into the general stress response regulatory network in Escherichia coli. *Journal of molecular microbiology and biotechnology* **4**, 341-346 (2002).

520   39.   Mangan MW, Lucchini S, Danino V, Croinin TO, Hinton JC, Dorman CJ. The integration host factor (IHF)
521   integrates stationary-phase and virulence gene expression in Salmonella enterica serovar Typhimurium. *Mol*
522   *Microbiol* **59**, 1831-1847 (2006).
523

524   40.   Martinez-Santos VI, Medrano-Lopez A, Saldana Z, Giron JA, Puente JL. Transcriptional regulation of the
525   ecp operon by EcpR, IHF, and H-NS in attaching and effacing Escherichia coli. *J Bacteriol* **194**, 5020-5033
526   (2012).
527

528   41.   Huang J, Chen S, Huang K, Yang L, Wu B, Peng D. [Identification of rpoE gene associated with biofilm
529   formation of Salmonella pullorum]. *Wei sheng wu xue bao = Acta microbiologica Sinica* **55**, 156-163 (2015).
530

531   42.   Baba T*, et al.* Construction of Escherichia coli K-12 in-frame, single-gene knockout mutants: the Keio
532   collection. *Mol Syst Biol* **2**, 2006.0008 (2006).
533

534   43.   Sambrook J. Molecular Cloning: A Laboratory Manual (ed^(eds). Cold Spring Harbor Laboratory (1989).
535

536   44.   Sperandio V, Torres AG, Kaper JB. Quorum sensing Escherichia coli regulators B and C (QseBC): a novel
537   two-component regulatory system involved in the regulation of flagella and motility by quorum sensing in E.
538   coli. *Mol Microbiol* **43**, 809-821 (2002).
539

540   45.   O'Toole GA. Microtiter dish biofilm formation assay. *Journal of visualized experiments : JoVE*, (2011).
541

542   46.   de Las Heras A, Xiao W, Sren V, Elfick A. Edwin. *SLAS technology* **22**, 50-62 (2017).
543

544   47.   Prigent-Combaret C*, et al.* Complex regulatory network controls initial adhesion and biofilm formation in
545   Escherichia coli via regulation of the csgD gene. *J Bacteriol* **183**, 7213-7223 (2001).
546

547   48.   Zhou Y, Smith DR, Hufnagel DA, Chapman MR. Experimental manipulation of the microbial functional
548   amyloid called curli. *Methods Mol Biol* **966**, 53-75 (2013).
549

550   49.   Cline MS*, et al.* Integration of biological networks and gene expression data using Cytoscape. *Nat Protoc* **2**,
551   2366-2382 (2007).
552

553   50.   Mika F, Hengge R. A two-component phosphotransfer network involving ArcB, ArcA, and RssB coordinates
554   synthesis and proteolysis of sigmaS (RpoS) in E. coli. *Genes Dev* **19**, 2770-2781 (2005).
555

556   51.   Hengge R. Proteolysis of sigmaS (RpoS) and the general stress response in Escherichia coli. *Res Microbiol*
557   **160**, 667-676 (2009).
558

559   52.   Jofré MR, Rodríguez LM, Villagra NA, Hidalgo AA, Mora GC, Fuentes JA. RpoS integrates CRP, Fis, and
560   PhoP signaling pathways to control Salmonella Typhi hlyE expression. *BMC Microbiol* **14**, 139 (2014).
561

562   53.   Mika F, Hengge R. Small Regulatory RNAs in the Control of Motility and Biofilm Formation in E. coli and
563   Salmonella. *Int J Mol Sci* **14**, 4560-4579 (2013).
564

565   54.   Pasemann F. Complex dynamics and the structure of small neural networks. *Network* **13**, 195-216 (2002).
566

567   55.   Grant SG, Jessee J, Bloom FR, Hanahan D. Differential plasmid rescue from transgenic mouse DNAs into
568   Escherichia coli methylation-restriction mutants. *Proc Natl Acad Sci U S A* **87**, 4645-4649 (1990).
569

570   56.   Datsenko KA, Wanner BL. One-step inactivation of chromosomal genes in Escherichia coli K-12 using PCR
571   products. *Proc Natl Acad Sci U S A* **97**, 6640-6645 (2000).
572

573   57.   Bachmann BJ. Pedigrees of some mutant strains of Escherichia coli K-12. *Bacteriol Rev* **36**, 525-557
574   (1972).
575
576

577
578
579
580
581
582

583 **Tables**

584 **Table 1.** Bacterial strains, plasmids and primers used in this study.

Strain	Description	Reference
E. coli DH5α	F⁻ *endA1 glnV44 thi-1 recA1 relA1 gyrA96 deoR nupG purB20* φ80d*lacZ*ΔM15 Δ(*lacZYA-argF*)U169, hsdR17($r_K^-m_K^+$), λ⁻.	[55]
E. coli BW25113	*lacI⁺rrnB*$_{T14}$ Δ*lacZ*$_{WJ16}$ *hsdR514* Δ*araBAD*$_{AH33}$ Δ*rhaBAD*$_{LD78}$ *rph-1* Δ*(araB–D)567* Δ*(rhaD–B)568* Δ*lacZ4787*(::*rrnB-3*) *hsdR514 rph-1*.	[56]
E. coli JW1702	*E. coli* BW25113 Δ*ihfA* mutant strain	[56]
E. coli JW3229	*E. coli* BW25113 Δ*fis* mutant strain	[56]
E. coli MG1655	*K-12 F– λ– ilvG– rfb-50 rph-1*	[57]
Plasmids		
pMR1	CmR, orip15a; GFPlva promoter probe vector	[27]
pMR1-Pj100	CmR, orip15a; pMR with synthetic constitutive promoter BBa_J23100	This study
pMR1-PrpoS	CmR, orip15a; pMR1-rpoS-GFPlva transcriptional fusion	This study
pMR1-PrpoE	CmR, orip15a; pMR1-rpoE-GFPlva transcriptional fusion	This study
pMR1-PcsgD	CmR, orip15a; pMR1-csgD-GFPlva transcriptional fusion	This study
pMR1-PflhD	CmR, orip15a; pMR1-flhD-GFPlva transcriptional fusion	This study
pMR1-PfliA	CmR, orip15a; pMR1-fliA-GFPlva transcriptional fusion	This study
pMR1-PyeaJ	CmR, orip15a; pMR1-yeaJ-GFPlva transcriptional fusion	This study
pMR1-PadrA	CmR, orip15a; pMR1-adrA-GFPlva transcriptional fusion	This study
pMR1-PcpxR	CmR, orip15a; pMR1-cpxR-GFPlva transcriptional fusion	This study
pMR1-PmatA	CmR, orip15a; pMR1-matA-GFPlva transcriptional fusion	This study
pMR1-PompR	CmR, orip15a; pMR1-ompR-GFPlva transcriptional fusion	This study
pMR1-PfliA/IHFmut	CmR, orip15a; pMR1-fliA/IHFmut-GFPlva transcriptional fusion	This study
pMR1-PyeaJ/Fismut	CmR, orip15a; pMR1-yeaJ/Fismut-GFPlva transcriptional fusion	This study
Primers	**Sequence**	
5 adrA EcoRI	5'-GCGCGAATTCCGAAAAAAGTTTGACGCCAC-3'	This study
3 adrA BamHI	5'-GCGCGGATCCCAATTTTCCCAAATTATAGAGACGG-3'	This study
3 adrA SphI	5'-GCGCGCATGCGCACGTTTACGCCCATTAC-3'	This study
5 cpxR EcoRI	5'-GCGCGAATTCGCGTGGCTTAATGAACTGAC-3'	This study
3 cpxR BamHI	5'-GCGCGGATCCTGTTTAAATACCTCCGAGGCA-3'	This study
3 cpxR SphI	5'-GCGCGCATGCATGAAGCAGAAACCATCAGATAG-3'	This study
5 matA EcoRI	5'-GCGCGAATTCTTTTCACTCAAACTGTTAAGATG-3'	This study
3 matA BamHI	5'-GCGCGGATCCCCGGAAGTAAATAAGATACGT-3'	This study
3 matA SphI	5'-GCGCGCATGCACCAATAATTTGCTAAGGCC-3'	This study
5 ompR EcoRI	5'-GCGCGAATTCCTCGTTGATTCCCTTTGTCT-3'	This study
3 ompR BamHI	5'-GCGCGGATCCGCAACAATTTGTAAGCGTGT-3'	This study
3 ompR SphI	5'-GCGCGCATGCCACCAGGTAACATTAAATCCAG-3'	This study
5 fliA - IHFmut overlap	5'-CCCGGGTTGCACATTCCCGGGGGCCGGATAAGGCGT-3'	This study
3 fliA - IHFmut overlap	5'-CCCCGGGAATGTGCAACCCGGGTAAATTGCAATTCAACTTGTAGGC-3'	This study
5 yeaJ -Fismut EcoRI	5'-GCGCGAATTCGAAGCGAAAAGCGAGGG-3'	This study

585 **Figure legends**

586

587 **Figure 1. General strategy to define novel regulatory interactions controlling planktonic/biofilm transition**.

588 The flagella-biofilm network was constructed and analyzed based on available data from the literature. Subsequently,

22

589   analysis of the promoter architecture regions of the principal nodes effectors was performed to confirm the

590   interactions reported. Next, cloning of the natural promoter regions in the pMR1-reporter system were developed.

591   Promoter activity was determined for each promoter in different conditions as established in material and methods.

592   Finally, GFP activity was transform into connectivity data and loaded into flagella-biofilm network to gain a better

593   understanding of this program.

594   **Figure 2. Flagella-biofilm transcriptional regulatory network**. The principal nodes and paths, which drive the

595   flagella-biofilm network were analyzed using Cytoscape 3.4.1. The network was analyzed by using betweenness

596   centrality and edge betweenness centrality algorithms [54]. Size of the nodes (circles) indicates betweenness analysis

597   and width of the Edges (lines connections the circles) indicates the edge betweenness analysis. Scale colors from

598   red to bright to dark indicate the high to low values.

599   **Figure 3. Effect of CRP, IHF and Fis GRs over the promoter activity of *rpoS*, *rpoE* and *flhD*.** Promoter activity

600   assay of (A) pMR1-P*rpoS,* (B) pMR1-P*rpoE,* and (C) pMR1-P*flhD* were evaluated in *E. coli* BW25113 *wild type* (blue

601   line), Δ*ihf* (red line) and Δ*fis* (green line) in 96well plate as described in methods in the absence (left panel) or

602   presence (right panel) of 0.4% of glucose. GFP fluorescence was measured each 20 minutes at 37 ºC during 8 hours

603   in static conditions and normalized by OD600. Solid lines represents the average from three independent

604   experiments while dashed lines are the upper and lower limits of standard error of the mean (S.E.M).

605   **Figure 4. Effect of CRP, IHF and Fis GRs on the promoter activity of *csgD*, *fliA* and *yeaJ*.** GFP promoter activity

606   assay of (A) pMR1-P*csgD,* (B) pMR1-P*fliA,* and (C) pMR1-P*yeaJ* were evaluated in *E. coli* BW25113 *wt* (blue line),

607   Δ*ihf* (red line) and Δ*fis* (green line) in 96well plate as described in methods in the absence (left panel) or presence

608   (right panel) of 0.4% of glucose. GFP fluorescence was measured each 20 minutes at 37 ºC during 8 hours in static

609   conditions and normalized by OD600. Solid lines represents the average from three independent experiments while

610   dashed lines are the upper and lower limits of standard error of the mean (S.E.M).

611   **Figure 5. Experimental data integration to the Flagella-biofilm transcriptional regulatory network**. Promoter

612   activity values were transformed into activation or repression connections and were loaded into Cytoscape 3.4.1. An

613   organic algorithm was used to the properly cluster visualization. The network was analyzed by use the betweenness

614   centrality and edge betweenness centrality measurements. Size of the nodes (circles) indicates betweenness

615   analysis and width of the Edges (lines connections the circles) indicates the edge betweenness analysis. Scale

616   colors from red to bright to dark indicate the high to low values.

617   **Figure 6. Effect of GRs in the motility program at 24h.** Motility phenotype of *E. coli* BW25113 wild-type and

618   mutant strains were evaluated by cell motility assay at 24h in the presence or absence of glucose as depicted.

619   Divergent motility capability is observed between the different conditions, proving the effect of the GRs CRP, IHF and

620   Cis to modulate the motility program. The results are representative of 3 independent experiments.

621   **Figure 7. Capability of *E. coli* and mutant strains to develop adherence and mature biofilm**. A) Adherence

622   capability of E. coli BW25113 *wild-type*, Δ*ihf* and Δ*fis* were evaluated in 96-well plate using violet crystal method.

623   Comparisons of adherence capability of BW25113 wt and mutant strains at 30 and 37˚C are shown. Vertical bars are

624   standard deviations calculated from three independent experiments. B) Mature biofilm formation of *E. coli* BW25113

625   *wt*, Δ*ihf* and Δ*fis* strains were perform using congo red plate assay. Comparisons of the mature biofilm morphological

626   characteristics of wild type and mutant strains at 37˚C in the presence or absence of glucose is shown. Dashed line,

627   Zone III; white line, zone II; black line, zone I; arrows represent wrinkles and clefts structures. The results are
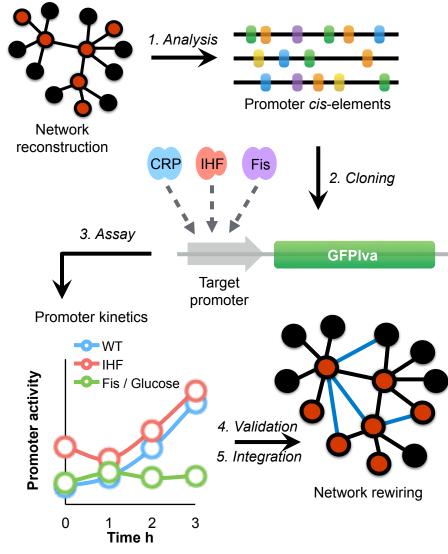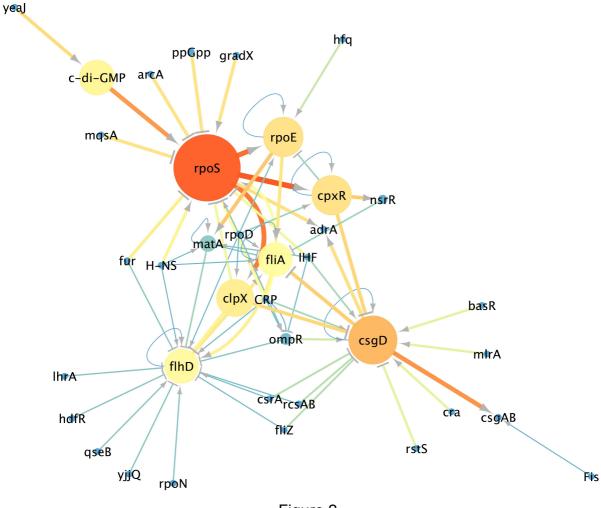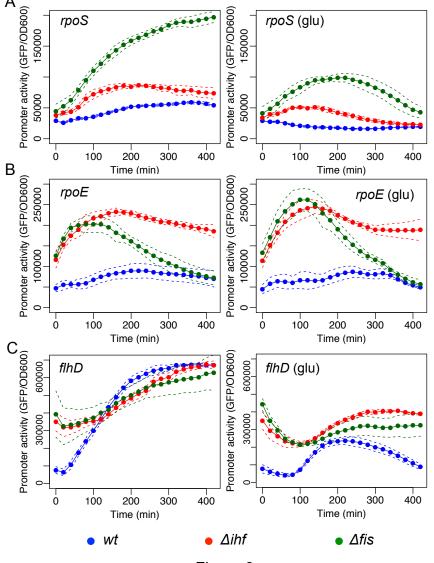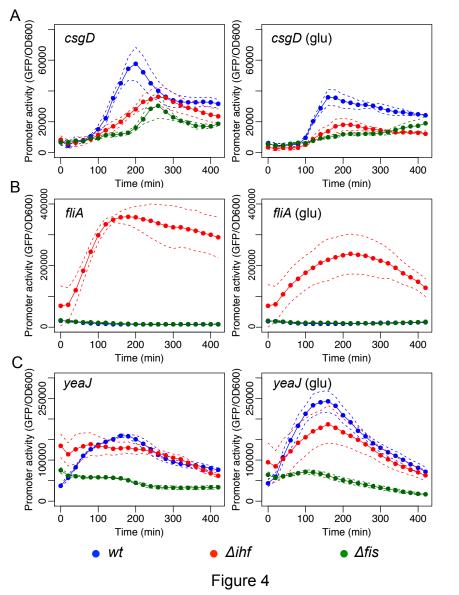
628   representative of 3 independent experiments.

1. Analysis

Network reconstruction

Promoter *cis*-elements

CRP   IHF   Fis

2. Cloning

3. Assay

Target promoter

GFPlva

Promoter kinetics

- WT
- IHF
- Fis / Glucose

Promoter activity

Time h

4. Validation

5. Integration

Network rewiring

Figure 1

Figure 2

Figure 3

Figure 4

Figure 5

Figure 6

Figure 7